

# Omni-Roach: A legged robot capable of traversing multiple types of large obstacles and self-righting

Jonathan Mi, Yaqing Wang, and Chen Li<sup>1</sup>

**Abstract**—Robots excel at avoiding obstacles but still struggle to traverse complex 3-D terrain with cluttered large obstacles. By contrast, insects like cockroaches excel at doing so. Recent research in our lab elucidated how locomotor transitions emerge from locomotor-environment interaction for diverse locomotor challenges abstracted for complex 3-D terrain and what strategies overcome these challenges. Here, we build on these fundamental insights to develop a cockroach-inspired legged robot, Omni-Roach, that integrates these strategies for multi-functional locomotion. The robot is based on the RHex-class design with six compliant legs and features a rounded body shape with two wings that can open, an active tail with pitch and yaw degrees of freedom. Through two development and testing iterations, our robot was capable of overcoming all locomotor challenges with high performance and success rate. It traversed cluttered rigid pillars only  $1.1\times$  robot body width apart, a  $2.5\times$  hip height bump, a  $0.75\times$  body length gap, densely cluttered flexible beams only  $65\%$  its body width apart, and self-righted within 4 seconds. Systematic experiments on tail use and approach angle for beam traversal revealed that an active tail pointed downward and tapping against the ground helps roll the body into the gap and break frictional and interlocking contact to traverse.

**Index Terms**—terradyamics, locomotion, multi-functional, bio-inspired robotics, biomimetics

## I. INTRODUCTION

Robots excel at navigating flat surfaces with sparse obstacles by creating a geometric map of the environment [2] and planning and following a collision free trajectory to avoid obstacles [3]–[6]. However, robots are still poor at traversing complex 3-D terrain cluttered with large obstacles, which requires physically interacting with obstacles rather than avoiding them. This has hindered important robot applications such as earthquake search and rescue in rubble [7], environmental monitoring on a forest floor [8], and extraterrestrial exploration through Martian rocks [9]. This lack of robot ability to traverse is largely due to a poor understanding of robot-terrain physical interaction [1]. By contrast, insects like cockroaches are excellent at doing this, often transitioning across different locomotor modes [10]. Understanding how they do so by using and controlling physical interaction with the environment can advance the ability of robots to do so.

Recent studies in our lab using an interdisciplinary terradyamics approach have begun to reveal how locomotor transitions in complex 3-D terrain emerge from physical interaction and how physical interaction can be controlled to modulate locomotor transitions [8]. This was achieved by systematic animal, robot, and physics studies of model systems of distinct locomotor challenges (Fig. 1b) abstracted from locomotion in complex 3-D terrain (Fig. 1a). For each model system, locomotor-environment interaction leads to stereotyped locomotor modes (Fig. 2a). Our physics models validated against animal and robot experiments revealed how a suite of

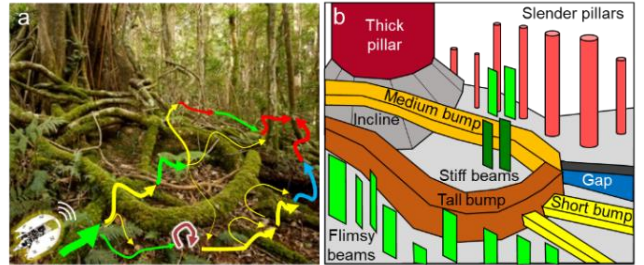


Fig. 1. Abstracting locomotor transitions in complex 3-D terrain with large obstacles. (a) Envisioned capability of robot traversing complex 3-D terrain. (b) Abstracted challenges from diverse large obstacles. Reproduced from [1].

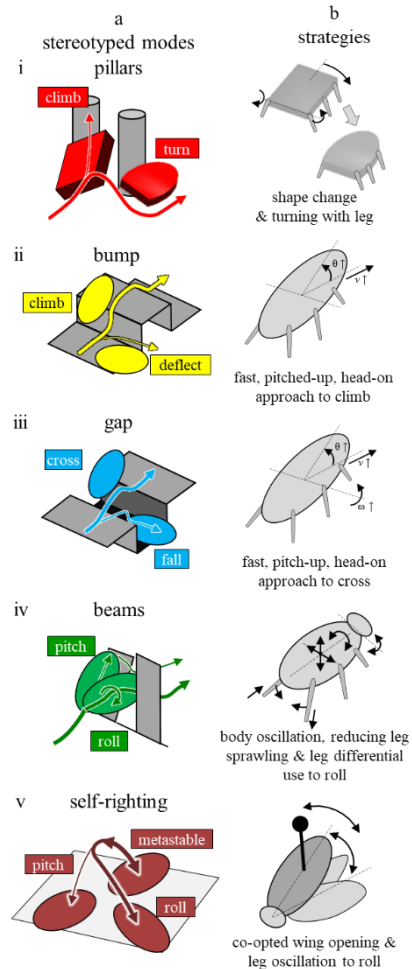


Fig. 2. Fundamental principles of strategies to overcome abstracted challenges. (a) Stereotyped modes discovered for each locomotor challenge. (b) Strategies to modulate locomotor transitions between modes to better overcome challenges. Adapted from [1].

design, actuation, and action strategies (Fig. 2b) can increase robot performance for each locomotor challenge by enhancing transition to desired modes or suppressing undesirable ones.

<sup>1</sup> Department of Mechanical Engineering, Johns Hopkins University. J.M. is with the Department of Electrical & Computer Engineering, University of California, San Diego and performed the research at JHU in an

Building on these foundations, here we take the next step towards robust robot traversal of complex 3-D terrain, by developing and testing a cockroach-inspired legged robot, Omni-Roach, capable of overcoming multiple locomotor challenges. Based on insights from each model system, we proposed how to integrate them in a single robot to achieve multi-functionality (Sec. II). We first developed and tested an initial prototype (Sec. III). Based on limitations revealed, we refined the robot and improved its performance of overcoming multiple locomotor challenges (Sec. IV). For traversing grass-like beam obstacles, a novel solution for traversal was developed, and further systematic experimentation was conducted to understand how to best use this solution (Sec. V). Finally, we review our contribution and discuss future directions (Sec. VI).

## II. DESIGN FOR MULTI-FUNCTIONALITY

We first review strategies to overcome the distinct locomotor challenges revealed by our previous studies to inform how to design and control a single robot to overcome these challenges. The robot is based on the classic RHex platform [11], with six legs spinning in an alternating tripod gait.

(i) To better traverse cluttered, rigid, large vertical obstacles such as pillars (Fig. 2, i) [12], a robot can simply adopt an elliptical body shape that passively repels it from obstacles to maintain a desired turn mode. By contrast, the cuboidal body common in robots is attracted to obstacles during self-propulsion and leads to an undesired climb mode.

(ii) To better traverse large horizontal obstacles with height increase like a bump (Fig. 2, ii) [13], a robot should move towards the bump rapidly, head-on, and pitch the body up to facilitate transitioning into a desired climb mode. An active tail with a pitch degree of freedom can be used to pitch the body up using inertial effect.

(iii) To better traverse large horizontal obstacles with height drop like a gap (Fig. 2, iii) [14], strategies similar to those for bump traversal facilitates transitioning to a desired cross mode, and an active tail is useful in a similar fashion.

(iv) To better traverse densely cluttered large, flexible obstacles such as grass-like beams (Fig. 2, iv), a robot should roll into a gap and maneuver through. This can be facilitated by a rounded ellipsoidal body [10], large body oscillations [15], and differential leg use and body flexion [16]. An ellipsoidal body helps lead the robot to align with and roll into the gap and reduce the potential energy barrier to move through it [10]. Large body oscillations provide kinetic energy fluctuation to help overcome the potential energy barrier [15]. Finally, differential leg use assists body rolling while body flexion breaks resistive frictional and interlocking contact between the body and edge of beams [16].

(v) To self-right after flipping over, a likely scenario when moving through large obstacles [10], [17] (Fig. 2, v), simultaneous wing opening and lateral leg oscillations facilitates transitioning from an undesired metastable body orientation to a desired roll mode that results in an upright orientation [18]–[21]. Wing opening lifts the center of mass and reduces the base of support formed by robot-ground contact points, reducing the potential energy barrier to self-right [18], [21], [22]. Lateral leg oscillations generate kinetic energy fluctuation that perturbs the body to overcome the barrier [21], [22].

Based on these insights, we identified three design features that can be integrated into a single robot for overcoming

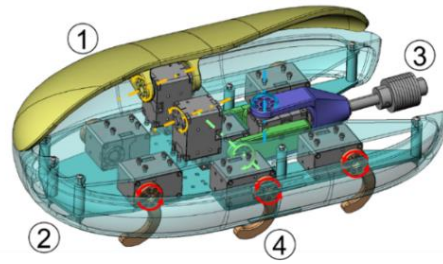


Fig. 3. Omni-Roach v1 CAD model. (1) Actuated wings that can open (left wing is not shown). (2) Fixed bottom shell. (3) Active 2-DOF tail. (4) Compliant C-shaped legs. Arrows show rotational joints, red for leg joints, yellow for wing joints, and green and blue for tail pitch and yaw joints, respectively.

multiple locomotor challenges. (1) A rounded body to help passively deflect the robot away from rigid vertical obstacles with no need for active control and roll into gaps to traverse densely cluttered flexible obstacles. (2) An active tail to pitch the body up for traversing large horizontal obstacles and to generate body oscillations for traversing densely cluttered flexible obstacles and self-righting. (3) The ability of the top shell of rounded body to open as wings for self-righting.

## III. INITIAL ROBOT DEVELOPMENT & TESTING

### A. Design

The first prototype, Omni-Roach v1 (Fig. 3), measures 35 cm long (excluding the tail), 23 cm wide, 13 cm tall, and weighs 1.8 kg, with a 5 cm hip height. The chassis plates were laser cut from acrylic. The six compliant C-shaped legs were 3D-printed from elastic thermoplastic polyurethane (TPU) filament. All other custom components were 3D-printed from polylactic acid (PLA) filament. Besides six servo motors that spin the legs (Fig. 3, red arrows), two motors actuate a tail with both pitch and yaw degrees of freedom (Fig. 3, green and blue arrows). The tail weighs 0.17 kg (9% of total body mass) and measures 19 cm (54% body length) from the pitch pivot axis to the tip. It is defined to be at home position (pitch = yaw = 0°) when the tail is pointing straight backwards (position shown in Fig. 3). The rounded body shell was divided into the top and bottom halves, with the top separated into the left and right halves, each capable of opening via rolling by a servo motor (Fig. 3, yellow arrows). We used DYNAMIXEL XL430-W250-T servo motors (no load speed 0.95 rev/s, stall torque 1.4 N·m) for all joints. The robot was controlled through a computer running a Python program with a TTL2USB interfacing device. The motors are set to operate at their maximum speed.

### B. Testing

We built simple testbeds to study the robot for each locomotor challenge (Fig. 4a-c). Each obstacle was mounted to a pegboard as the ground (Fig. 4a-d). The pillar (Fig. 4a) was an aluminum bar vertically fixed to the ground. The bump obstacle (Fig. 4b) was constructed by stacking square aluminum bars so that bump height can be varied. Sandpaper (60 grit) was fixed to the ground to improve leg traction. The beams were acrylic plates (6 mm thick) mounted on the ground via a joint with torsion springs [23]. We chose a high torsional stiffness of  $k = 0.78 \text{ N}\cdot\text{m}/\text{rad}$  so that the robot was unable to simply push over the beams to traverse. In all trials, the robot was manually controlled.

### C. Performance

#### 1) Pillar traversal

The rounded body enabled Omni-Roach v1 to deflect away and traverse pillars (Fig. 5, a) 100% of the time without any active control.

#### 2) Bump traversal

Without tail use, Omni-Roach v1 was unable to pitch its body sufficiently by simply pushing against the bump and was deflected away (Fig. 5b, iii). With tail use, the robot pitched up to climb over the bump (Fig. 5b, i-ii) before it deflected. Initially, it only traversed a maximal bump height of  $1\times$  hip height. This was because the rear end of the long top and bottom shell contacted the ground during body pitching, causing the rear legs to lose ground contact and diminishing propulsion. By clipping off the rear end of top and bottom shell (Fig. 5b, i, red circle) to reduce chassis-ground contact, Omni-Roach v1 traversed a bump of up to  $1.5\times$  hip height with an 80% success rate.

#### 3) Gap traversal

Omni-Roach v1 traversed a 17 cm gap (48% body length) without tail actuation. This was not improved with tail actuation. This was due to the slow spinning leg motors, limiting the robot speed to below the necessary speed for dynamic gap traversal. The slow tail motor also did not generate sufficient body pitching via inertial effects.

#### 4) Beam traversal

Without tail use, Omni-Roach v1 pitched up against the beams and became stuck during self-propulsion, unable to traverse (Fig. 5c, iii). By keeping the tail pitched downward and manually yawing it left and right at roughly 2 Hz, the tail pushed against the ground and helped the body roll, which, together with intermittent leg propulsion against the beams, enabled the robot to traverse (Fig. 5c, i-ii). Similar to how cockroaches adjust their legs and abdomen to traverse the beams [16] and a recent robot [24], the robot's tail tapping and intermittent leg propulsion worked together to oscillate the robot and break the frictional and interlocking contact with the beams. By varying beam gap width, we found that Omni-Roach v1 was capable of traversing beams with a gap 91% of the robot body width (or a 21 cm gap, Fig. 9d). To quantify how much the body rolled to achieve this, we estimated the approximate maximal body roll. Neglecting body thickness:

$$\text{body roll} = \cos^{-1} \frac{\text{beam gap}}{\text{body width}} \quad (1)$$

To traverse the gap of 91% body width, the robot rolled by approximately  $24^\circ$ . Beam traversal probability and its dependence on tail mode and approach angle was further studied in Sec. V.

#### 5) Self-righting

Omni-Roach v1 self-righted by opening the wings to raise the body and keeping the tail pitched downward (relative to the body) and yawing it to one side (Fig. 5d, i). After the robot rolled onto its side, the wings were closed and the tail moved back to the home position (Fig. 5d, ii). The wing contacting the ground further pushed the robot upright (Fig. 5d, iii). The self-righting was robust with a 90% success rate and within 4 s on flat ground.

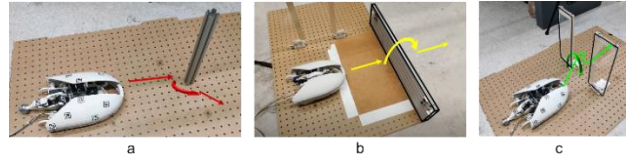


Fig. 4. Simple terrain testbeds. (a) Pillar. (b) Bump. (c) Beams. Colored arrows show favored locomotor modes, with colors following those in Fig. 1.

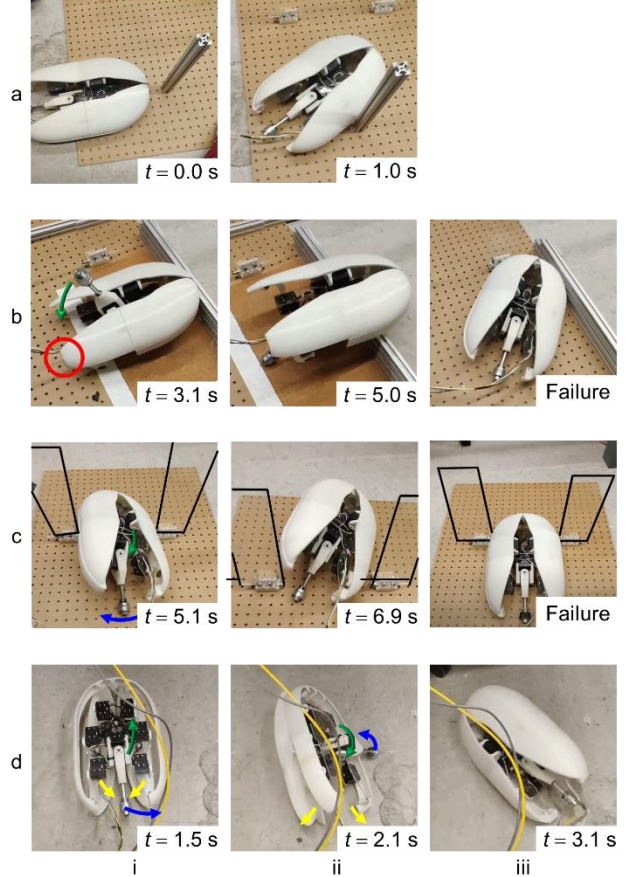


Fig. 5. Snapshots of Omni-Roach v1 overcoming locomotor challenges. (a) Pillar. (b) Bump of  $1.5\times$  hip height. Red circle shows the clipped-off wings and bottom chassis. (c) Beams with a 91% body width gap. (d) Self-righting. Blue and green arrows show tail yaw and pitch motions. Yellow arrows show wing motions.

### D. Limitations revealed

Omni-Roach v1 was capable of completing the bump, pillar, beam, and self-right challenges. However, the performance of the robot on the bump, beam, and gap could be improved. We speculated that the performance could be improved by further reducing the size and weight of the robot to make it more agile. Tail usage was important for bump and beam traversal, so improvements to the tail could be impactful. Improvements to the legs could also enable better forward propulsion.

## IV. REFINED ROBOT DEVELOPMENT & TESTING

### A. Design

Learning from the results of Omni-Roach v1, we developed Omni-Roach v2 (Fig. 6) to further improve performance. Omni-Roach v2 measures 20 cm long (excluding the tail), 18.5 cm wide, 10 cm tall, and weighs 0.75 kg. The hip height is same as Omni-Roach v1 at 5 cm. Overall, Omni-

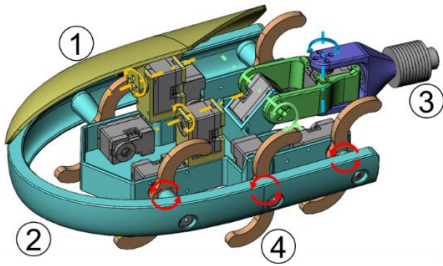


Fig. 6. Omni-Roach v2 CAD model. (1) Actuated wings that can open (left wing is not shown). (2) Fixed bottom shell. (3) Active 2-DOF tail. (4) Compliant S-shaped legs. Arrows show rotational joints, red for leg joints, yellow for wing joints, and green and blue for tail pitch and yaw joints, respectively.

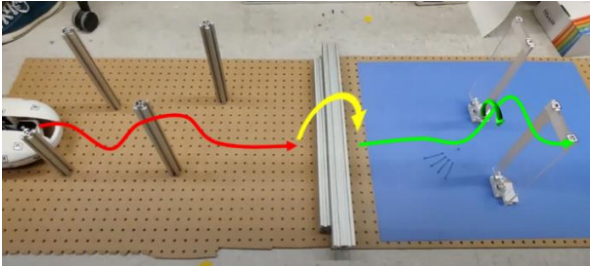


Fig. 7. Multi-obstacle field with four pillars, a bump, and two beams. Colored arrows show favored locomotor modes, with colors following those in Fig. 1.

Roach v2 is about two thirds the size of v1 (Fig. 9a) and less than half the weight, making it much more agile. Despite the shortened and flatter chassis, leg length remains the same, giving the legs more reach relative to body size. The tail weighs 0.1 kg (13% of total body mass) and measures 14.5 cm (73% body length) from the pitch pivot axis to the tip. The tail home position is defined the same way as in v1 (position shown in Fig. 6). The tail was lengthened relative to body length to reduce chassis-ground contact which hindered bump traversal. We used the smaller, lighter, and faster DYNAMIXEL XL330-M288-T servo motors (no load speed 1.71 rev/s, stall torque 0.52 N·m). The legs were also changed from C- to S-shape to further double stride frequency. The motors operated at maximum speed in all experiments.

### B. Multi-obstacle testbed

Besides testing for each type of obstacle like for v1, to demonstrate Omni-Roach v2's ability to traverse complex terrain with multiple types of challenges, we created a multi-obstacle field (Fig. 7) consisting of four pillars spaced 20 cm, a bump obstacle, and a pair of beams. The robot was controlled to traverse through this course and then was manually flipped over to perform self-righting (multimedia material).

### C. Performance

#### 1) Pillar traversal

The rounded body enabled Omni-Roach v2 to deflect away 100% of the time from the pillar (Fig. 8a) without any active control.

#### 2) Bump traversal

The same traversal strategy as Omni-Roach v1 was utilized for Omni-Roach v2. With tail use, Omni-Roach v2 pitched up to climb over a maximal bump height of  $2.5\times$  hip height (Fig. 8b, i-ii) with an 80% success rate.

#### 3) Gap traversal

Omni-Roach v2 traversed a 13.5 cm gap (68% body length) with the tail stowed in the body and a 15 cm gap (75%

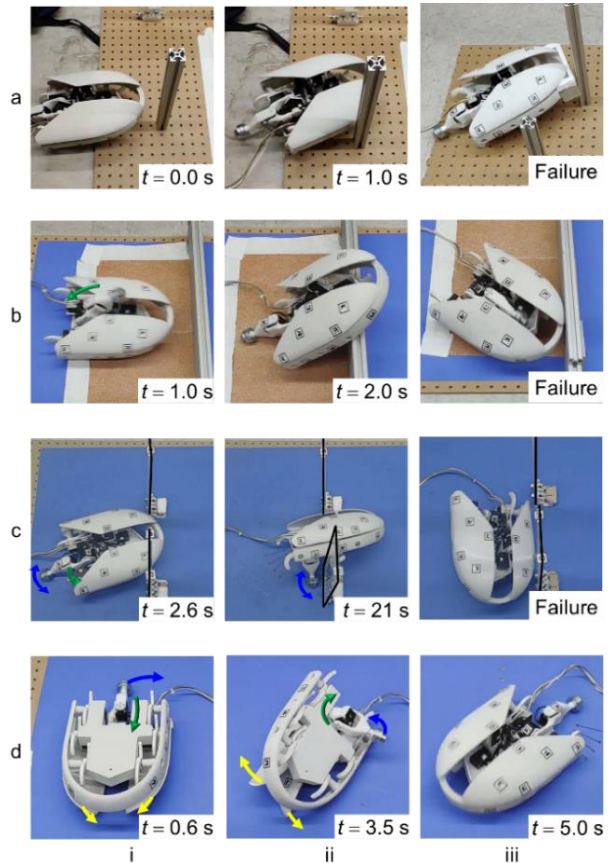


Fig. 8. Snapshots of Omni-Roach v2 overcoming locomotor challenges. (a) Pillar. (b) Bump of  $2.5\times$  hip height. Red circle shows the clipped-off wings and bottom chassis. (c) Beams with a 65% body width gap. (d) Self-righting. Blue and green arrows show tail yaw and pitch motions. Yellow arrows show wing motions.

TABLE I  
COMPARISON BETWEEN OMNI-ROACH V1 AND V2

	v1	v2
Length (cm)	35	20
Width (cm)	23	18.5
Height (cm)	13	10
Weight (kg)	1.8	0.75
Hip height (cm)	5	5
Pillar traversal probability	100%	100%
Maximum bump height ( $\times$ hip height)	1.5	2.5
Maximum gap length ( $\times$ body length)	48%	75%
Roll angle to traverse beams (deg)	24	50
Self-right time (sec)	4	4

body length) with the tail in the home position to help bridge the gap. Despite Omni-Roach v2 being smaller, lighter, and faster, the performance still cannot be improved by involving a tail motion. The leg and tail motors are still too slow to generate sufficient forward kinetic energy and sufficient body pitching to dynamically traverse as in [14].

#### 4) Beam traversal

Omni-Roach v2 utilizes the same techniques as Omni-Roach v1 to traverse the beams. By varying beam gap width, we found that Omni-Roach v2 was capable of traversing beams (Fig. 8c, i-ii) with a gap only 65% of the robot body width (or a 12 cm, Fig. 9e). This translates to approximately a  $50^\circ$  body roll. Beam traversal of the Omni-Roach v2 is further discussed in Sec. V.

### 5) Self-right performance

Omni-Roach v2 self-righted (Fig. 8d, i-iii) utilizing the same sequence as Omni-Roach v1, taking only 4.0 s with a 100% success rate on flat ground.

### D. Comparison to v1

A comparison of size and performance between Omni-Roach v1 and v2 is listed in Tab. 1. Omni-Roach v2 had a higher performance in bump and gap traversal, capable of traversing a bump of  $2.5\times$  hip height compared to  $1.5\times$  for v1 (Fig. 9b-c) and a gap of 75% body length compared to 48% for v1. It also had a better performance in beam traversal, capable of rolling into the beams by  $50^\circ$  to traverse a 65% body width gap, compared to rolling by  $24^\circ$  to traverse a 91% body width gap for v1 (Fig. 9d-e). It maintained the same level of performance in pillar traversal and self-righting.

This performance increase was mainly due to the increase in the relative leg length (from 14% to 25% body length) and relative tail length (from 54% to 73% body length), while maintaining relative leg propulsion (single leg stall force/body weight only slightly reduced from 1.6 to 1.4). In addition, Omni-Roach v2 has a stride frequency about 4 times that of v1, which generated more oscillations during beam interaction and better perturbed the body to break frictional and interlocking contact.

### V. TAIL USE FOR BEAM TRAVERSAL

Among challenges of pillars, bump, beams, and self-righting, we observed that cluttered beam traversal required the most finesse of coordination between tail pitch and yaw, taking the longest to complete and appearing to depend sensitively on beam approach angle. In addition, a recent study of a RHex-class robot traversing uneven terrain discovered that by introducing downward tail tapping to perturb the body, the robot can be freed from being stuck in uneven terrain [24]. We speculate that similar active tail tapping can perturb our robot out of being stuck when pushing against the beams by breaking frictional and interlocking contact. During testing we noticed that at some approach angles the robot would become stuck in the beams. Considering these, we further studied how tail use and approach angle affect beam traversal of Omni-Roach v2.

#### A. Experimental setup and procedure

To challenge the robot in this experiment, we used a beam gap of 65% robot body width (or 12 cm). We tested four tail operation modes. (1) Home static: a static tail with  $0^\circ$  pitch and  $0^\circ$  yaw relative to the chassis (Fig. 10a). (2) Pitch down static: a static tail pointing downward, with  $90^\circ$  pitch and  $0^\circ$  yaw relative to the chassis (Fig. 10b). (3) Pitch down and yaw static: a static tail pointing downward and sideways, with  $90^\circ$  pitch and  $15^\circ$  yaw relative to the chassis (Fig. 10c). (4) Pitch down with yaw oscillation: a downward pointing, laterally oscillating tail, with  $90^\circ$  pitch relative to the chassis and a manually controlled yaw oscillation from  $-15^\circ$  to  $15^\circ$  at 2 Hz (Fig. 10d). These mode choices are inspired from a beam traversal experiment with a cockroach[25]. When the animal first rolled into the gap, it flexed its abdomen down (abdomen pitched from  $7^\circ$  to  $37^\circ$  relative to the body) and oscillated the abdomen to propel itself forward. In (4) pitch down with yaw oscillation tail mode, the tail pitch resembles

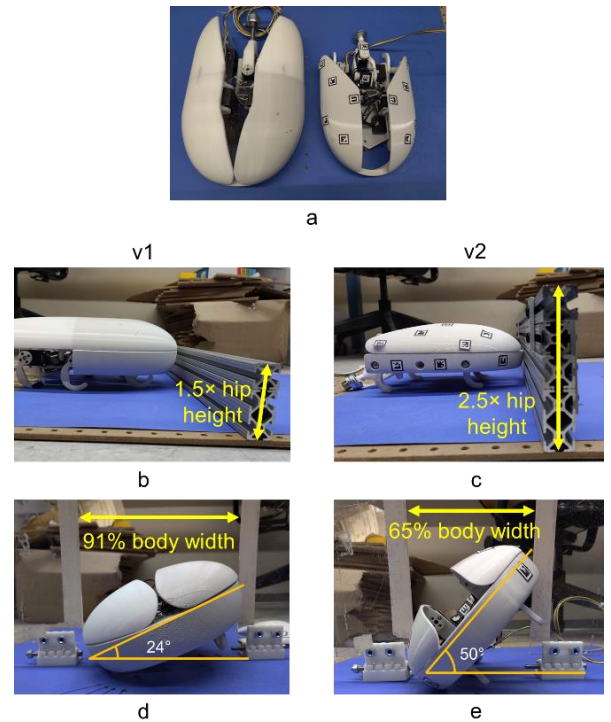


Fig. 9. Comparison between Omni-Roach v1 (left) and v2 (right). (a) Top view of robots. (b-c) Bump of maximal height traversed. (d-e) Gap of minimal gap traversed, showing maximal body roll achieved.

the abdomen pitch and the yaw oscillation resembles the abdomen oscillation in the animal experiment. The other modes were chosen to compare with (4).

We varied approach angle, the angle between the midline of the two beams to the midline of the robot (Fig. 10e), from  $0^\circ$  to  $45^\circ$  in increments of  $15^\circ$ . With everything else kept the same, we collected 10 trials for each combination of tail mode and approach angle, resulting in a total of 160 trials.

#### B. Results

Traversal probability depended sensitively on tail operation mode (Fig. 11a). In the home static tail mode, Omni-Roach v2 could not traverse at any approach angle because the small roll perturbation from leg propulsion was insufficient to roll the body into the gap. Instead, the robot pitched up and oscillated against the beams and became trapped.

In the pitch down and yaw static tail mode, the robot was also unable to traverse at any approach angle. Although the statically yawed tail rolled the robot body, the resistance between the body and beams prevented the robot from fully entering the gap. As a result, the robot was deflected away 75% of the time and trapped between the beams 25% of the time.

In the pitch down static tail mode, Omni-Roach v2 was unable to traverse at a  $0^\circ$  approach angle but did so with a high probability at the  $15^\circ$ ,  $30^\circ$ , or  $45^\circ$  approach angles. At  $0^\circ$  approach angle, the robot head could not fully enter the gap, which caused it to become stuck or deflected away. At larger approach angles, the head entered the gap, which led to body rolling that enabled traversal.

In the pitch down with yaw oscillation tail mode, the robot was able to traverse at all four approach angles with a high probability. The oscillating tail tapped against the ground, which served two functions. First, it rolled the body substantially and helped it enter the gap. Second, it generated perturbations to break frictional and interlocking contact to free the

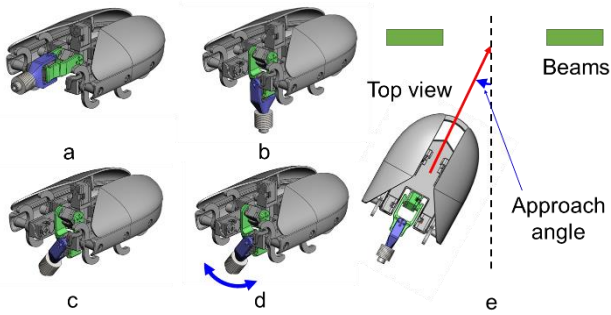


Fig. 10. Experimental design to study the effects of tail use and approach angle for beam traversal. Four tail modes tested: (a) Home static. (b) Pitch down static. (c) Pitch down and yaw static. (d) Pitch down with yaw oscillation. Arrows show yaw oscillation. (e) Definition of approach angle.

body from being stuck when maneuvering through the gap. As a result, traversal time (Fig. 11a) of the pitch down with yaw oscillation tail mode was reduced by an average of 30% from that of the pitch down static tail mode at 15°, 30°, or 45° approach angles ( $****P < 0.001$ , ANOVA).

We further compared average traversal time between different tail modes where the robot traversed at a high probability, defined as the time from when the robot first touched the beams to when the robot fully left the beams after traversal through the gap. (Fig. 11b). The robot traversed more quickly using the pitch down with yaw oscillation tail mode than the pitch down static tail mode at all approach angles ( $P < 0.001$ , repeated-measures ANOVA). Traversal time also reduced with approach angle ( $***P < 0.01$ , ANOVA).

We noted that, without tail oscillation, a static tail that pitched downward to support the body could allow the robot to roll into the gap and traverse, but only when the approach angle is appropriate. Thus, we speculated that one function of tail oscillation is to adjust the approach angle. This is consistent with our animal observation [25] that cockroaches flexed their abdomen (like a tail pitching down) and oscillated it (like a tail yawing left and right) when traversing a cluttered layer of beams.

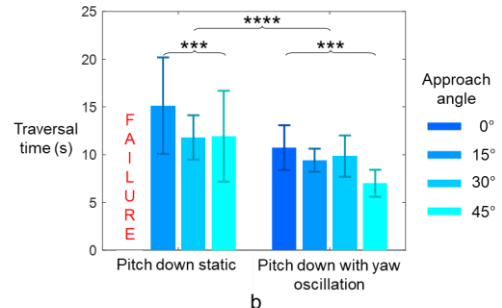
## VI. SUMMARY & FUTURE WORK

We developed and tested a small, multi-functional legged robot that can traverse multiple types of large obstacles and self-right, tasks that are required for effective operation complex 3-D terrain. Through two development and testing iterations, our robot can traverse a field of cluttered rigid pillars with  $1.08\times$  body width gaps via passive interaction without sensing and feedback control, traverse a large bump  $2.5\times$  its hip height, a large gap  $0.75\times$  its body length gap, and densely cluttered beams with gaps  $65\%$  its body width with active tail use, and self-right within 4.0 s. Systematic experiments showed that the robot traversed beams with a high probability with appropriate tail use.

Our work opens opportunities for several further directions. (1) Motor/transmission and tail improvements to enable dynamic gap traversal and improve bump traversal. With smaller and faster motors (as in [13], [14]), we can make the robot even lighter and generate a higher speed approaching a gap or bump. Increasing the tail weight relative to the robot driven by a sufficiently powerful motor can enhance body pitching. Both of these will increase gap and bump traversal performance [13], [14]. (2) Redesigning leg geometry. Robot propulsion could be improved with leg geometry changes

	Approach angle				Probability
	0°	15°	30°	45°	
Home static	0%	0%	0%	0%	
Pitch down static	0%	90%	90%	70%	
Pitch down and yaw static	0%	0%	0%	0%	
Pitch down with yaw oscillation	70%	100%	90%	100%	

a



b

Fig. 11. Beam traversal performance of Omni-Roach v2. (a) Traversal probability. (b) Average traversal time of successful trials for different approach angles for pitch down static (left) and pitch down with yaw oscillation (right) tail modes.

such as minitour-like legs [26] or GOAT legs [27]. This could better enable gap traversal by having a longer leg length that gives a larger initial speed, and beam traversal by actively adjust the legs to reduce leg resistance. (3) Body shape morphing. Although it helps traverse pillars and beams, the rounded shell deflects the robot away from the bump and hinders traversal. To overcome this, a shape morphing shell [28] could be developed to use a cuboidal body to turn towards large bumps to facilitate climbing [12]. (4) Autonomous locomotor transitions. The current robot is manually controlled to transition between locomotor modes. By closing the loop with vision and contact force sensors [29] to detect the geometry and physical properties [22] of large obstacles and developing an algorithm to control the robot to change actuation to switch modes, autonomous traversal of complex 3-D terrain can be achieved.

Finally, considering our findings on tail use in beam traversal, it would be intriguing to study how cockroaches sense terrain resistance and control its body flexion and leg adjustment to quickly slither through dense vegetation [16]. Our lab is developing a robotic physical model with contact force sensing and feedback control to adjust body rotation and flexion to study this systematically [22], [25].

## ACKNOWLEDGMENT

J.M. thanks Qihan Xuan and Ratan Othayoth for discussion and the Laboratory for Computational Sensing & Robotics (LCSR) of the Johns Hopkins University for hosting his REU. We thank Xiao Yu for naming the robot. This work was supported by an Arnold & Mabel Beckman Foundation Beckman Young Investigator Award and a Burroughs Wellcome Fund Career Award at the Scientific Interface to C.L. and an NSF research experience for undergraduates (REU) award hosted by JHU LCSR to J.M. Author contributions: J.M. designed robots, performed experiments, and wrote the paper; Y.W. analyzed data, provided feedback on robot design and experiment, and revised the paper; C.L. oversaw study and revised the paper.

## REFERENCES

- [1] R. Othayoth et al., ‘Locomotor transitions in the potential energy landscape-dominated regime’, *Proc. R. Soc. B Biol. Sci.*, vol. 288, no. 1949, p. rspb.2020.2734, 2021.
- [2] M. E. Jefferies and W.-K. Yeap, ‘Simultaneous Localization and Mapping’, in *Robot and cognitive approaches to spatial mapping*, vol. 38, Springer, 2008, pp. 13–42.
- [3] J. Borenstein and Y. Koren, ‘The vector field histogram-fast obstacle avoidance for mobile robots - Robotics and Automation, IEEE Transactions on’, *IEEE Trans. Robot.*, vol. 7, no. 3, pp. 278–288, 1991.
- [4] O. Khatib, ‘Real-time obstacle avoidance for manipulators and mobile robots’, in *Autonomous Robot Vehicles*, New York: Springer, 1986, pp. 396–404.
- [5] E. Rimon and D. E. Koditschek, ‘Exact robot navigation using artificial potential functions’, *IEEE Trans. Robot. Autom.*, vol. 8, no. 5, pp. 501–518, 1992.
- [6] S. Thrun, ‘Toward robotic cars’, *Commun. ACM*, vol. 53, no. 4, pp. 99–106, 2010.
- [7] F. Matsuno et al., ‘Utilization of Robot Systems in Disaster Sites of the Great Eastern Japan Earthquake’, in *Field and Service Robotics*, Springer, 1998, pp. 1–18.
- [8] G. Freitas et al., ‘Design, modeling, and control of a wheel-legged locomotion system for the environmental hybrid robot’, *Proc. 2nd IASTED Int. Conf. Robot. Robo 2011*, pp. 302–310, 2011.
- [9] L. Matthies et al., ‘Computer Vision on Mars’, *Int. J. Comput. Vis.*, vol. 75, no. 1, pp. 67–92, Jul. 2007.
- [10] C. Li et al., ‘Terradynamically streamlined shapes in animals and robots enhance traversability through densely cluttered terrain’, *Bioinspiration and Biomimetics*, vol. 10, no. 4, p. 46003, 2015.
- [11] U. Saranli et al., ‘RHex: A Simple and Highly Mobile Hexapod Robot Recommended Citation RHex: A Simple and Highly Mobile Hexapod Robot’, pp. 616–631, 2001.
- [12] Y. Han et al., ‘Shape-induced obstacle attraction and repulsion during dynamic locomotion’, 2021.
- [13] S. W. Gart and C. Li, ‘Body-terrain interaction affects large bump traversal of insects and legged robots’, *Bioinspir. Biomim.*, vol. 13, no. 2, p. 026005, Feb. 2018.
- [14] S. W. Gart et al., ‘Dynamic traversal of large gaps by insects and legged robots reveals a template’, *Bioinspir. Biomim.*, vol. 13, no. 2, p. 026006, Feb. 2018.
- [15] R. Othayoth et al., ‘An energy landscape approach to locomotor transitions in complex 3D terrain’, *Proc. Natl. Acad. Sci. U. S. A.*, vol. 117, no. 26, pp. 14987–14995, 2020.
- [16] Y. Wang et al., ‘Uncovering the role of head flexion during beam obstacle traversal of cockroaches’, *Integr. Comp. Biol.* 61, no. Meeting Abstracts, 2021.
- [17] C. Li et al., ‘Mechanical principles of dynamic terrestrial self-righting using wings’, *Adv. Robot.*, vol. 31, no. 17, pp. 881–900, 2017.
- [18] Q. Xuan, ‘Randomness in appendage coordination facilitates strenuous’, *Bioinspir. Biomim.*, vol. 15, no. 6, p. 65004, 2020.
- [19] Q. Xuan and C. Li, ‘Coordinated Appendages Accumulate More Energy to Self-Right on the Ground’, vol. 5, no. 4, pp. 6137–6144, 2020.
- [20] C. Li et al., ‘Cockroaches use diverse strategies to self-right on the ground’, *J. Exp. Biol.*, vol. 222, no. 15, 2019.
- [21] R. Othayoth and C. Li, ‘Propelling and perturbing appendages together facilitate strenuous ground self-righting’, *Elife*, vol. 10, pp. 1–23, 2021.
- [22] Q. Xuan et al., ‘Environmental force sensing enables robots to traverse cluttered obstacles with interaction’, *IEEE Robot. Autom. Lett.*, 2021.
- [23] Q. Xuan and C. Li, ‘A potential energy landscape based dynamic model of locomotion in complex 3-D terrain’, *Bull. Am. Phys. Soc.* 66, vol. S14, no. Meeting Abstracts, p. 006, 2021.
- [24] D. Soto et al., ‘Enhancing Legged Robot Navigation of Rough Terrain via Tail Tapping’, 2022, pp. 213–225.
- [25] Y. Wang et al., ‘A robophysical model to study physical sensing of obstacles in legged traversal of complex 3-D terrain’, *Bull. Am. Phys. Soc.* 66, vol. S14, no. Meeting Abstracts, p. 007, 2021.
- [26] G. Kenneally et al., ‘Design Principles for a Family of Direct-Drive Legged Robots’, *IEEE Robot. Autom. Lett.*, vol. 1, no. 2, pp. 900–907, 2016.
- [27] S. Kalouche, ‘Design for 3d agility and virtual compliance using proprioceptive force control in dynamic legged robots’, Master’s thesis, Carnegie Mellon University, Pittsburgh, PA, 2016.
- [28] S. Mintchev and D. Floreano, ‘Adaptive morphology: A design principle for multimodal and multifunctional robots’, *IEEE Robot. Autom. Mag.*, vol. 23, no. 3, pp. 42–54, 2016.
- [29] S. Sundaram et al., ‘Learning the signatures of the human grasp using a scalable tactile glove’, *Nature*, 2019.

[Supplementary Movie.](#)